Pseudo-shock system structure in rectangular Laval nozzles with gaps

T. Gawehn[1], M. Giglmaier[2], J. F. Quaatz[2], A. Gülhan[1], and N. A. Adams[2]

1 Introduction

The acceleration of a fluid in a Laval nozzle to supersonic speed leads to a significant decrease of the static temperature in the flow, and deceleration via a normal shock results in a sudden reheating. Both effects are used within the joint project PAK 75 (Deutsche Forschungsgemeinschaft DFG) for the homogeneous ignition of a precursor and, hence, for the production of gas phase synthesized nanoparticles with narrow size distribution. However, the shock boundary layer interaction at the desired shock position leads to the formation of a so-called pseudo-shock system. Thereby, the heating rate across the shock system is reduced and the homogeneity of the particle growth is negatively affected by the inhomogeneous downstream conditions. Such pseudo-shock systems have been investigated by many research groups and a comprehensive overview is given by [1].
A necessity for many investigations is optical access to the flow. To avoid stresses within the quartz glass side walls, the windows have to be mounted with small gaps of $\Delta z = O(10^{-4})$ m. As it has been shown already in [2], these gaps result in small bypass mass flows which play a significant role in presence of high pressure gradients (e.g. critical cross sections and shocks).
The objective of the current investigation is an experimental analysis on the effect of bypass mass flow on the pseudo-shock system for different gap sizes. Additionally, numerical simulations performed by the Institute of Aerodynamics and Fluid Mechanics are used to verify the observed phenomena.

[1] *Institute of Aerodynamics and Flow Technology, Supersonic and Hypersonic Technology Department, German Aerospace Center (DLR), Linder Höhe, 51147 Cologne, Germany*
[2] *Lehrstuhl für Aerodynamik und Strömungsmechanik, Technische Universität München Boltzmannstrasse 15, 85748 Garching, Germany*

2 Experimental Tools

The experiments are carried out at a fully automated DLR test rig in Cologne. The test rig allows stagnation pressures p_{01} up to 54 bar, stagnation temperatures T_{01} up to 800 K and mass flow rates $\dot{m}_{01}$ up to 1.5 kg/s. The test conditions are set and controlled by a process control system. The accuracy level of the stagnation conditions is better than $\pm 1\%$ for the stagnation temperature T_0 and $\pm 0.5\%$ for the stagnation pressure p_0.

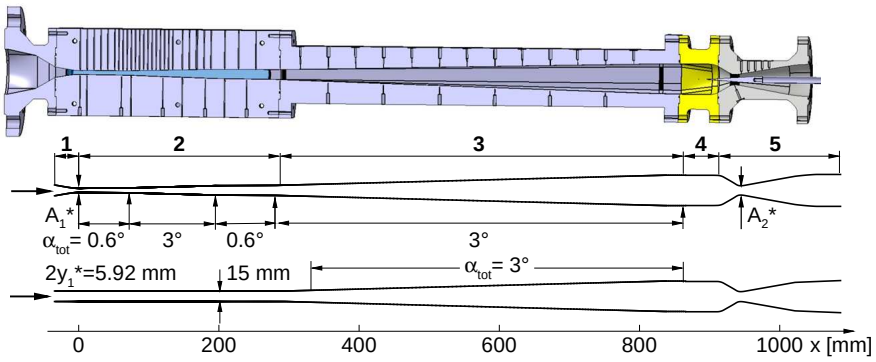

Fig. 1 Geometry of the test rig in Colone

The geometry of the test rig is shown in fig. 1. Within the primary nozzle ① and ②, the flow is accelerated to supersonic flow speed. The location of the shock system within the divergent part ② of the first Laval nozzle is defined by the cross sectional area of the second critical nozzle throat ⑤ and can be controlled by a slender movable cone. For determining the flow conditions, static pressure taps are placed on the top wall of the whole system. The modular primary nozzle can be equipped with optical access on both parallel side walls. Metallic side walls with additional pressure taps for dynamic pressure measurements can be used instead. The downstream conditions of the shock system can be analyzed in the doubly divergent reactor part ③ by means of thermocouples in the flow and pressure taps on the top wall.

In order to analyze the influence of the gap size between the quartz glass side walls and the metal structure of the facility, three different set-ups of the modular primary nozzle are investigated. A sketch of the channel cross section is given in fig. 2. The gap size between the nozzle contour and the side wall can be varied by adding some aluminium sealing. Investigations with approximately 0.0 mm gap (fig. 2a) are performed with metallic side walls without flow visualization. Further tests are performed with quartz glass windows with 0.1 mm (fig. 2b) and 0.2 mm gap width (fig. 2c) . By increasing the gap size to 0.2 mm, the channel half width is increased to 7.6 mm.

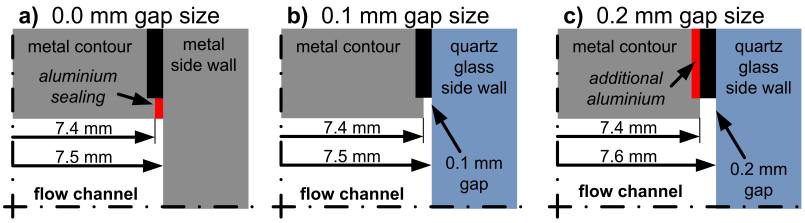

Fig. 2 Cut-view at $x = \text{const.}$ of the analyzed gap configurations

3 Investigation techniques and test procedure

The static wall pressure distribution is recorded with miniature Electronic Pressure Scanners (Esterline ESP-32 HD®) of the PSI System 8400 and Ethernet Intelligent Pressure Scanners (Model 9116 EIPS®). In total, 80 static wall pressures can be recorded simultaneously with an accuracy of better than ± 3.5 mbar. For dynamic pressure measurements five XTL-IA-140M® of Kulite Semiconductor with an accuracy of better than ± 6.8 mbar are used.
Flow visualization is performed with a Z-type schlieren system with spherical mirrors of 150 mm in diameter using an 11 Megapixel monochromatic PROSILICA GE4000 CCD-Kamera and a 50 ns flash lamp. Thereby, the small scale structures of the complex pseudo-shock system can be timely resolved.
For the computation of the flow, the commercial fluid dynamics solver Ansys CFX is used by the Institute of Aerodynamics and Fluid Mechanics. The 3-D time dependent Favre-averaged Navier-Stokes equations for compressible flow are combined with an explicit algebraic Reynolds stress turbulence model (EARSM) to resolve secondary flows such as corner vortices in square cross sections. Further details on the simulation can be found in [3].
The flow is controlled by setting the stagnation conditions (p_{01}, T_{01}) upstream of the primary nozzle and by adjusting the position of the central body in the secondary nozzle throat, i.e. changing the pressure downstream of the primary nozzle. Thereby, different stagnation pressure ratios p_{02}/p_{01} across the pseudo-shock system can be investigated whereas p_{02} indicates the total pressure right upstream of the secondary nozzle, measured at about $x = 900$ mm downstream of the primary nozzle throat A_1^*.

4 Test results

Effect of gap size on the wall pressure distribution

The effect of the gap size on the pseudo-shock system structure has been investigated at different stagnation conditions (p_{01}, T_{01}) and different stagnation pressure ratios p_{02}/p_{01}. Using experiments at $p_{01} = 6.0$ bar and $T_{01} = 300$ K the main effects

will be analyzed by means of the recorded static wall pressure distribution.
In fig. 3 experimental data for different gap sizes at stagnation pressure ratios $p_{02}/p_{01} = 0.7$ (3a) and $p_{02}/p_{01} = 0.6$ (3b) are presented together with the numerical simulations at $p_{02}/p_{01} = 0.7$ (3c). Figure 3d shows dynamic pressure measurements for a gap size of 0.1 mm at both stagnation pressure ratios.

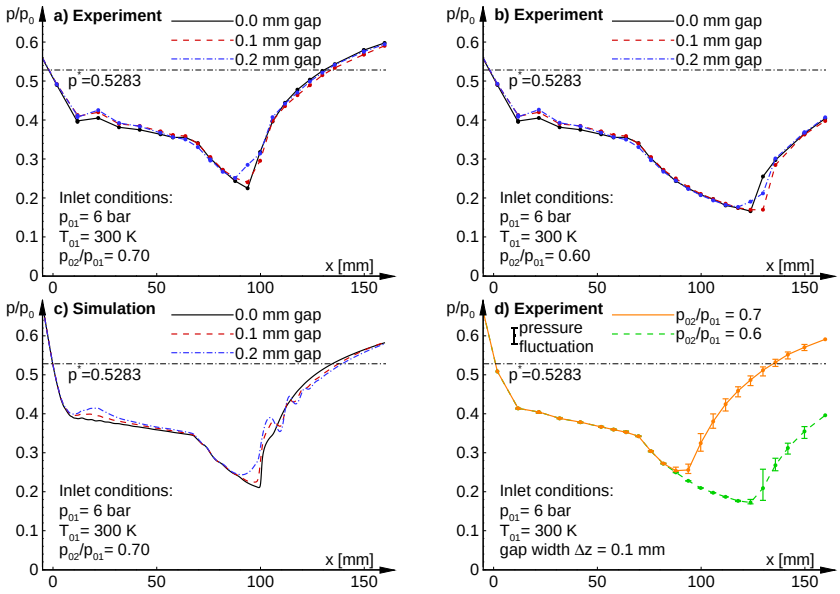

Fig. 3 Pressure distribution along the upper nozzle wall

Each plot in fig. 3a-c shows three curves. The solid black line represents the 0.0 mm gap size, the dashed red line represents the 0.1 mm gap size, and the dash-dotted blue line corresponds to the 0.2 mm gap size. As mentioned before, the gap flow mainly affects the pressure distribution in regions of high pressure gradients. Therefore, downstream of the primary nozzle throat at $x = 0$ mm the static pressure increases with increasing gap size and reaches a local maximum at $x = 22$ mm. The numerical simulations show, that a small bypass mass flow enters the gap shortly upstream of the critical cross section and re-enters into the shear flow of the supersonic part shortly downstream. This leads to a deceleration of the flow and thus to an increase of the static pressure. An obvious difference between the experiments and the simulations is the local maximum of the pressure at $x = 22$ mm. This local peak occurs in the experiment even without noticeable gap and was not reproduced by numerical simulations with exactly 0.0 mm gap size. We assume that the 0.0 mm gap size was not exactly achieved in the experiment.
A significant impact of the gap size on the main flow can be observed at the shock location. The high pressure gradient leads to a reverse flow through the gaps into the supersonic part ahead of the pseudo-shock system. In case of $p_{02}/p_{01} = 0.7$

both, experiment (fig. 3a) and simulation (fig. 3c), show a a static-pressure increase slightly upstream of the shock. A comparable pre-compression is observed for the stagnation pressure ratio $p_{02}/p_{01} = 0.6$ (fig. 3b). In this test case, the experiment shows a downstream shift of the shock. For proper explanation of this particular behavior, numerical simulations with $p_{02}/p_{01} = 0.6$ are currently in preparation.
Figure 3d shows the time averaged pressure distribution measured by the Kulite®-Sensors for the configuration with 0.1 mm gap size and stagnation pressure ratios of $p_{02}/p_{01} = 0.6$ (green, dashed) and 0.7 (orange, solid). Maxima and minima are indicated by error bars. For both stagnation pressure ratios, the pressure fluctuations in the supersonic part upstream of the pseudo-shock system are negligible. Within the shock system, the high initial fluctuations decay with increasing static pressure. High fluctuations in the pseudo-shock system and the mixing region indicate an axial oscillation of the shock position. This agrees with previous investigations where a streamwise oscillation of the shock system by several millimeters was observed by high speed schlieren visualization [2].

Visual analysis of the pseudo-shock system structure for different gap sizes

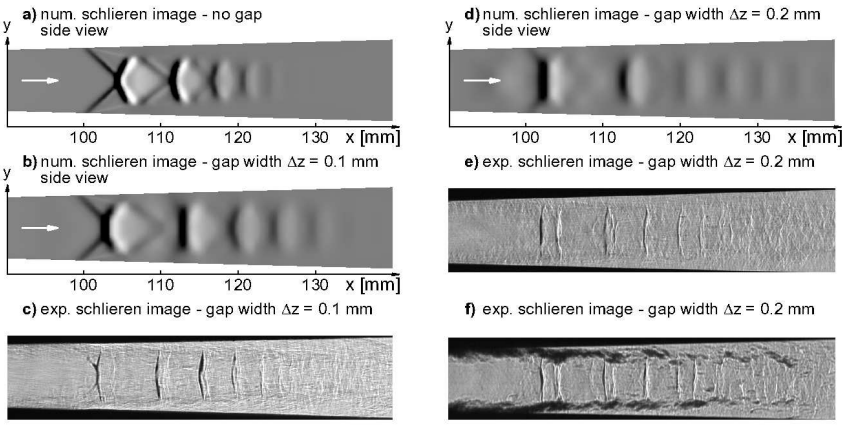

Fig. 4 Numerical and experimental schlieren pictures of the pseudo-shock system

For analysis of the structure of the pseudo-shock system, numerical and experimental schlieren images are used. Unfortunately, an experimental visualization for 0.0 mm gap size has not been achieved, but the numerical schlieren image in fig. 4a shows clearly the series of successive shocks (black) and expansion regions (white). The initial shocks form an x-configuration at the center line followed by a rarefaction region where the flow is re-accelerated until the next re-compression follows. The interaction of these shocks and rarefaction waves with the boundary layer results in its local thickening and, hence, in the formation of a virtual nozzle throat

that allows the flow to re-accelerate from subsonic to supersonic conditions.
The numerical and experimental schlieren images for a gap size of 0.1 mm are shown in fig. 4b and fig. 4c. In comparison to the simulation with 0.0 mm gap, the x-configuration on the center line is now deformed and a Mach disk with a normal shock at the center is observed. The boundary layers at the upper and lower wall remain much thinner and the length of the shock system is increased. The following shock structures are deformed to single normal shocks. A significant difference between the experimental and the numerical schlieren image is the observed and predicted distance between the first and the second shock.
For an assessment of the configuration with 0.2 mm gap a numerical schlieren image is shown in fig. 4d. Again, the compression is indicated in black, expansions are indicated in white. One observes that a strong expansion occurs directly downstream of the first shock. The following shocks show a similar, but much weaker behavior. The corresponding experimental schlieren image is depicted in fig. 4e. The first normal shock (black) is followed by a strong expansion (white). To investigate the origin of this rarefaction another schlieren image is depicted in fig. 4f. Unlike the previous image, this one is created by using a horizontal slit instead of a knife edge. With this technique the boundary layer is clearly visible. One observes that the separated boundary layers form the previously mentioned virtual new nozzle where the subsonic core flow is accelerated again to supersonic conditions.

5 Conclusion

A detailed experimental investigation of the influence of small gaps on a pseudo-shock system has been performed for different gap sizes and pressure ratios p_{02}/p_{01}. Since schlieren images only provide integral information of the total light deflection through the test section, 3-D numerical data was additionally used to investigate 3-D phenomena of the shock system. The combination of experimental and numerical techniques considerably increased the understanding of the underlying mechanisms that cause the change in structure and position of the pseudo-shock system when increasing the gap size.

References

1. K. Matsuo, Y. Miyazato and H.-D. Kim: Shock train and pseudo-shock phenomena in internal gas flows. In: *Progress in Aerospace Sciences, vol 35-1*, (1999)
2. T. Gawehn, A. Gülhan, M. Giglmaier, N.S. Al-Hasan and N.A. Adams: Analysis of Pseudo-Shock System Structure and Asymmetry in Laval Nozzles with Parallel Side Walls. In: *19th Interantional Shock Interaction Symposium*, Moscow (2010)
3. M. Giglmaier, J.F. Quaatz, T. Gawehn, A. Gülhan, and N.A. Adams: Numerical and experimental investigation of the effect of bypass mass flow due to small gaps in a transonic channel flow. In: *28th International Symposium on Shock Waves*, Manchester (2011)